RESEARCH FRONT

CSIRO PUBLISHING

Aust. J. Chem. **2013**, *66*, 1189–1201
http://dx.doi.org/10.1071/CH13157

Full Paper

Contrasting Reactivity of Mono- versus Bis-2,2,6,6-tetramethylpiperidide Lithium Aluminates Towards Polydentate Lewis Bases: Co-Complexation Versus Deprotonation

Ross Campbell,[A] *Elaine Crosbie,*[A] *Alan R. Kennedy,*[A] *Robert E. Mulvey,*[A,B] *Rachael A. Naismith,*[A] *and Stuart D. Robertson*[A,B]

[A]WestCHEM, Department of Pure and Applied Chemistry, University of Strathclyde, Glasgow, G1 1XL, UK.
[B]Corresponding authors. Email: r.e.mulvey@strath.ac.uk; stuart.d.robertson@strath.ac.uk

Two closely related lithium alkylaluminium amides LiAl(TMP)$_2$^{i}Bu$_2$ and LiAl(TMP)^{i}Bu$_3$ (TMP: 2,2,6,6-tetramethylpiperidide) have been compared in their reactivity towards six polydentate Lewis bases containing either N or O donor atoms or a mixed N,O donor set. Seven of the twelve potential organometallic products of these reactions, which were carried out in hexane solution, have been crystallographically characterised. Three of these structures, [Li(μ-Me$_2$NCH$_2$CHCH$_2$CH$_2$CHO)(μ-TMP)Al(^{i}Bu)$_2$], [Li(μ-Me$_2$NCH$_2$CH$_2$OCH$_2$)(μ-TMP)Al(^{i}Bu)$_2$], and [Li(μ-Me$_2$NCH$_2$CH$_2$OCHCH$_2$NMe$_2$)(μ-TMP)Al(^{i}Bu)$_2$] reveal that the bis-amide LiAl(TMP)$_2$^{i}Bu$_2$ deprotonates (aluminates) the multifunctional Lewis base selectively at the carbon atom adjacent to oxygen with the anion generated captured by the residue of the base. In contrast, the mono-amide LiAl(TMP)^{i}Bu$_3$ in general fails to deprotonate the Lewis bases but instead forms co-complexes with them as evidenced by the molecular structures of [Me$_2$NCH$_2$CHCH$_2$CH$_2$CH$_2$O·Li(μ-^{i}Bu)(μ-TMP)Al(^{i}Bu)$_2$], [Me$_2$NCH$_2$CH$_2$OMe·Li(μ-^{i}Bu)(μ-TMP)Al(^{i}Bu)$_2$], and [MeOCH$_2$CH$_2$OMe·Li(μ-^{i}Bu)(μ-TMP)Al(^{i}Bu)$_2$]. Providing an exception to this pattern, the mono-amide reagent deprotonates chiral *R*,*R*,-*N*,*N*,*N*′,*N*′-tetramethylcyclohexanediamine to afford [Li(μ-CH$_2$NMeC$_6$H$_{10}$NMe$_2$)$_2$Al(^{i}Bu)$_2$], the final complex to be crystallographically characterised. All new products have been spectroscopically characterised through ^{1}H, ^{7} Li, and ^{13}C NMR studies. Reaction mixtures have also been quenched with D$_2$O and analysed by ^{2}D NMR spectroscopy to ascertain the full metallation versus co-complexation picture taking place in solution.

Manuscript received: 5 April 2013.
Manuscript accepted: 27 May 2013.
Published online: 3 July 2013.

Introduction

Ubiquitous in synthetic chemistry for priming molecules for their subsequent functionalisation, the metallation reaction has traditionally been the domain of polar, highly reactive alkali-metals, notably lithium.[1–5] However, this discipline has evolved recently such that the place vacated on the molecule by the departing hydrogen atom can be *directly* taken by a less polar, less reactive metal such as magnesium, zinc, or manganese(II).[6–8] This is achieved by pairing such a metal with a polar alkali-metal within a discrete molecular bimetallic 'ate' framework, the result being that the alkali-metal in effect imparts its reactivity onto the subordinate metal which ultimately performs the deproto-metallation reaction. Since the subordinate metal cannot typically perform the metallation reaction by itself, the term 'alkali-metal-mediated metallation' was coined to reflect the subsidiary but mandatory role played by the group 1 metal in activating the less reactive metal.

Due to the high natural abundance, low toxicity, and relative inexpensiveness of aluminium, we have recently taken an interest in developing and understanding its role as the subordinate metal.[9] Organoaluminium chemistry, both in its +3 oxidation state, and more recently in its +1 state[10–12] has been comprehensively studied for many years. As a tri-valent metal, this opens up alternative potential reaction pathways when compared with the more often studied bi-valent metals mentioned above due to either the electronic effect of using a formal 3+ metal or the steric effects of introducing a further anion to saturate this increase in positive charge. In particular, our interest has focussed on the bis-amido/bis-alkyl heterobimetallic aluminate of general formula D·LiAl(TMP)$_2$^{i}Bu$_2$ (**1**, where D = a neutral Lewis donor molecule and TMP = 2,2,6,6-tetramethylpiperidide), which is generated in a facile manner by simply mixing equimolar quantities of Li(TMP) with (TMP)Al^{i}Bu$_2$ in hexane.[13] Aluminate **1** has been shown to act as an excellent chemoselective, halogen tolerant base towards functionalised aromatic substrates.[14,15]

Our studies have run in parallel with the excellent work of Uchiyama, Wheatley and coworkers who pioneered and have concentrated on the more alkyl-rich lithium aluminate LiAl(TMP)^{i}Bu$_3$ (**2**), which is also accessed through the

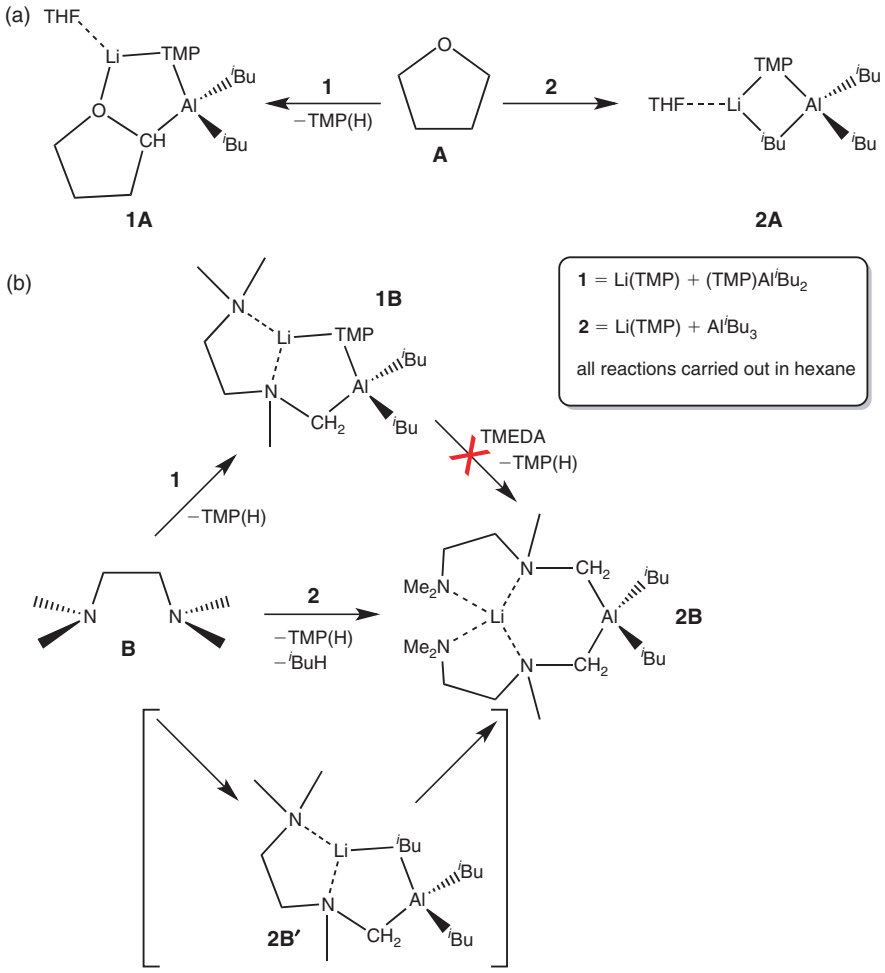

Scheme 1. Contrasting reactivity of aluminate bases **1** and **2** towards (a) THF and (b) *N*,*N*,*N*′,*N*′-tetramethylethylenediamine (TMEDA).

co-complexation of homometallic starting materials Li(TMP) and Al^{i}Bu$_3$.[16–18] What has consistently been clear throughout the study of these two closely related bimetallic bases is the difference in their reactivity upon the substitution of one of the alkyl groups in **2** by another equivalent of the bulky secondary amide in **1**. While both bases can operate in a 'conventional' manner with respect to functionalised aromatic molecules – that is they are potent direct aluminators (C–H to C–Al exchangers) of such molecules by the well established and understood principles of directed *ortho*-metallation (DoM)[19–21] – they display marked differences in their reactivity towards non-aromatic, heteroatom containing molecules. This is best displayed by their respective reactivities towards the most common cyclo-ether tetrahydrofuran (THF, donor **A**; Scheme 1a). Thus **2** can be stabilised as a THF solvate (**2A**)[22] and is routinely utilised in this medium;[17] while in contrast **1** will deprotonate THF at the methylene group adjacent to the heteroatom by TMP basicity, sedating the resulting highly sensitive cyclic anion (in **1A**)[23] without the ether cleavage typically witnessed when a monometallic approach to THF α-deprotonation is attempted.[24–26] Another pertinent example of the contrasting reactivity of aluminates **1** and **2** involves the common bidentate donor *N*,*N*,*N*′,*N*′-tetramethylethylenediamine (TMEDA, donor **B**).[27] While both bases will directly aluminate this diamine at one methyl group adjacent to the nitrogen atom, **2** will actually metallate a second equivalent to give **2B** as depicted in Scheme 1b. This distinction suggests that the first deprotonation event carried out by **2** must occur through TMP and not ^{i}Bu basicity to give intermediate **2B′** (which cannot be isolated), since if the latter situation was operative then this would generate complex **1B**, which is inert towards a further equivalent of TMEDA.

Interestingly, the solvent plays an important role in any reaction of a base such as **2** as demonstrated by its reaction with *N*,*N*-diisopropylbenzamide (Scheme 2). In hexane, a simple donor adduct (**2**·benzamide) is produced with no deprotonation;[28] whereas in THF *ortho*-deprotonation of the aromatic substrate results in a 94% yield of 2-iodo-*N*,*N*-diisopropylbenzamide after iodination.[16] When the hexane reaction is repeated in the presence of stoichiometric THF only a negligible amount of *ortho*-deprotonation occurs, while stoichiometric TMEDA yields a product which contains both deprotonated TMEDA and benzamide bridges as well as a ligating neutral benzamide.[29] Furthermore, **2**·benzamide will cleave 1,4-dioxan and capture the resulting highly sensitive alkoxy vinyl ether anion;[28] while **2** (in the absence of benzamide) produces the segregATE (solvent-separated ate) $[Li(dioxan)_4]^+$ $[Al(^iBu)_4]^-$, presumably from a dismutation process (Scheme 2).[30]

The captivating reactivity of alkali-metal aluminates is not limited to lithium derivatives, as exposed by the potassium

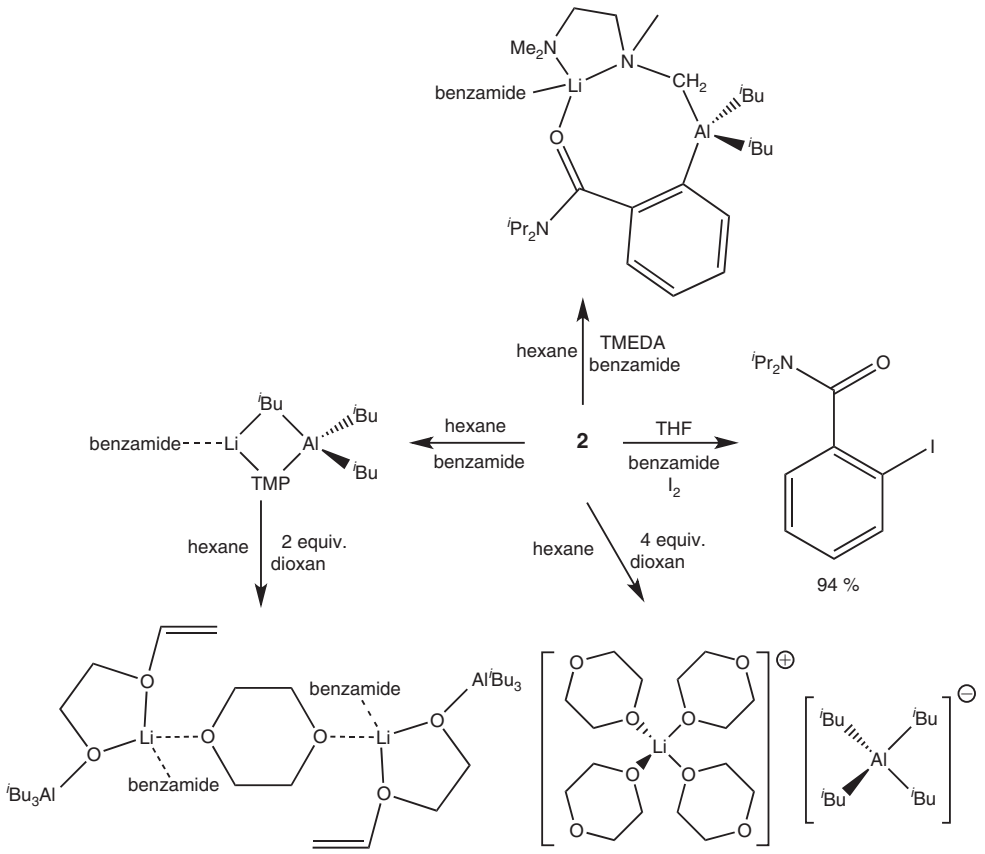

Scheme 2. Reactivity of aluminate **2** in hexane or THF with benzamide and dioxane.

aluminate congener $KAl(TMP)_2{}^iBu_2$ which, rather than attacking a neutral Lewis donor through TMP basicity, actually attacks the other TMP anion at a flanking methyl position to give an unprecedented *N*,*C*-bis-deprotonated TMP dianion, essentially inverting the TMP anion from a potent Brønsted base to a Brønsted acid.[31]

Intrigued by the vagaries in reactivity displayed by the two closely related lithium aluminates **1** and **2**, we have systematically studied their reactivity with a series of multidentate nitrogen and oxygen containing donor molecules **C**–**H** (shown in Fig. 1) that offer a variety of donor ligation and/or deprotonation possibilities in an attempt to further understand these important heterometallic reagents and now present our findings herein.

Experimental

General Experimental

All reactions and manipulations were carried out under a protective argon atmosphere using either standard Schlenk techniques or a glove box. All solvents were dried over Na/benzophenone and freshly distilled before use. $^iBu_2Al(TMP)$ and Li(TMP) were prepared in situ; *N*,*N*-dimethyltetrahydrofurfurylamine (Me_2TFA),[32] 1-methoxy-2-dimethylaminoethane (MDAE),[32] tris(*N*,*N*-dimethyl-2-aminoethyl) amine (Me_6TREN),[33] and *R*,*R*,*N*,*N*,*N*′,*N*′-tetramethylcyclohexanediamine (TMCDA)[34] were prepared by literature methods. Bis[2-(*N*,*N*-dimethylamino)ethyl]ether (Me_4AEE), $^iBu_3Al$ (1.0 M in hexane), and 1,2-dimethoxyethane (DME) were purchased from Aldrich and used as received. ^1H, ^{13}C, and ^7Li NMR spectra were recorded on a Bruker AV400 MHz spectrometer (operating at 400.03 MHz for ^1H, 100.58 MHz for ^{13}C, and 155.50 MHz for ^7Li). All ^{13}C NMR spectra were proton decoupled. Ligands containing a * next to their name indicate that they have been deprotonated and are in an anionic form. The high sensitivity of the organometallic species **1** and **2** prevented us from

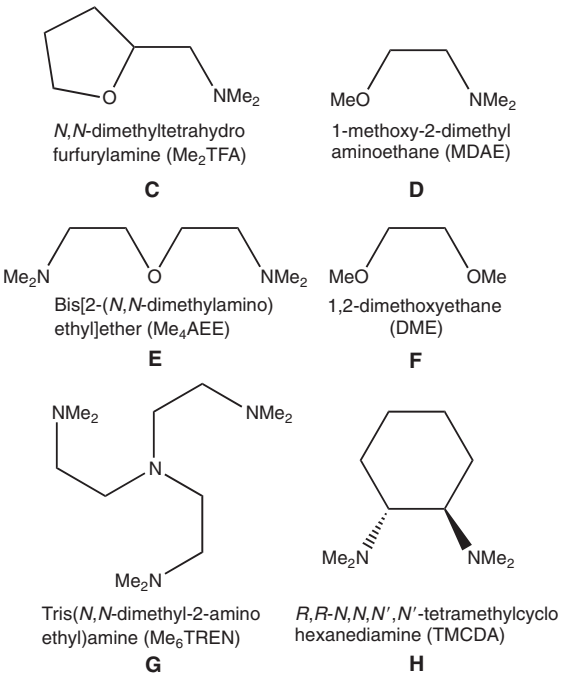

Fig. 1. Neutral heteroatom containing molecules employed in this study.

obtaining satisfactory elemental analyses. ^{1}H NMR spectra are provided in the Supplementary Material to confirm purity.

Synthesis of [Li(μ-TMP)(μ-Me$_2$TFA)Al(^{i}Bu)$_2$]* **1C**

Hexane (10 mL) was injected into an oven-dried Schlenk tube. Next, 1.6 M *n*BuLi (1.25 mL, 2 mmol) was added, followed by TMP(H) (0.34 mL, 2 mmol) at room temperature. The reaction mixture was left to stir for 10 min and then ^{i}Bu$_2$AlCl (0.38 mL, 2 mmol) was introduced, producing a white suspension almost immediately. The reaction was left to stir for 1 h and was then filtered through Celite and glass wool, which was then washed with more hexane (10 mL). To a separate Schlenk tube containing a solution of freshly prepared LiTMP in hexane (10 mL) (from a mixture of *n*BuLi (1.25 mL, 2 mmol) and TMP(H) (0.34 mL, 2 mmol)), the solution of ^{i}Bu$_2$Al(TMP) was added through a cannula. Finally, Me$_2$TFA (0.28 mL, 2 mmol) was added by injection and the reaction mixture was left to stir overnight. The solution was then left to stand in the freezer at −30°C. A crop of colourless crystals (0.24 g, 29 %) formed in solution, which were successfully studied by X-ray crystallographic analysis. Two diastereoisomers were observed by ^{1}H NMR spectroscopy in a ratio of 2 : 1 (diastereomer A : diastereomer B).

Diastereomer A: δ_H (400.13 MHz, THF-D$_8$, 298 K) −0.17 (1H, d, ^3J(H, H) 6.5, CH$_2$ of ^{i}Bu), −0.08 (3H, d, ^3J(H, H) 6.3, CH$_2$ of ^{i}Bu), 0.92 (12H, m, CH$_3$ of ^{i}Bu), 1.23 (1H, m, γCH$_2$ of TMP), 1.25 (6H, s, CH$_3$ of TMP), 1.27 (1H, m, AlCHC*H*$_2$ of Me$_2$TFA*), 1.30 (6H, s, CH$_3$ of TMP), 1.51 (1H, m, AlCHCH$_2$C*H*$_2$ of Me$_2$TFA*), 1.64 (1H, m, γCH$_2$ of TMP), 1.79 (1H, m, AlCHCH$_2$C*H*$_2$ of Me$_2$TFA*), 1.90 (2H, m, CH of ^{i}Bu), 1.92 (1H, m, AlCHC*H*$_2$ of Me$_2$TFA*), 2.06 (1H, m, C*H*$_2$NMe$_2$ of Me$_2$TFA*), 2.24 (6H, s, CH$_3$ of Me$_2$TFA*), 2.33 (1H, m, C*H*$_2$NMe$_2$ of Me$_2$TFA*), 3.26 (1H, dd, ^3J(H, H) 13.0, ^4J(H, H) 5.9, AlCH of Me$_2$TFA*), 3.94 (1H, m, C*H*CH$_2$N of Me$_2$TFA*).

Diastereomer B: δ_H (400.13 MHz, THF-D$_8$, 298 K) 0.00 (4H, m, CH$_2$ of ^{i}Bu)], 0.89 (12H, m, CH$_2$ of ^{i}Bu), 1.22 (6H, s, CH$_3$ of TMP), 1.24 (6H, s, CH$_3$ of TMP), 1.27 (1H, m, γCH$_2$ of TMP), 1.28 (1H, m, AlCHCH$_2$C*H*$_2$ of Me$_2$TFA*), 1.29 (1H, m, AlCHC*H*$_2$ of Me$_2$TFA*), 1.58 (1H, m, γCH$_2$ of TMP), 1.85 (2H, m, CH of ^{i}Bu), 1.95 (1H, m, AlCHCH$_2$C*H*$_2$ of Me$_2$TFA*), 2.05 (1H, m, AlCHC*H*$_2$ of Me$_2$TFA*), 2.17 (1H, m, C*H*$_2$NMe$_2$ of Me$_2$TFA*), 2.23 (6H, s, CH$_3$ of Me$_2$TFA*), 2.43 (1H, m, C*H*$_2$NMe$_2$ of Me$_2$TFA*), 3.37 (1H, dd, ^3J(H, H) 12.6, ^4J(H, H) 5.8, AlCH of Me$_2$TFA*), 3.98 (1H, m, C*H*CH$_2$N of Me$_2$TFA*). Due to the presence of several overlapping signals the βCH$_2$ of TMP could not be identified.

Diastereomer A: δ_C (100.62 MHz, THF-D$_8$, 298 K) 19.2 (γCH$_2$ of TMP), 28.0 (CH of ^{i}Bu), 28.1 (CH of ^{i}Bu), 32.8 (AlCHCH$_2$**C**H$_2$ of Me$_2$TFA*), 33.7 (CH$_3$ of TMP), 44.6 (AlCH**C**H$_2$ of Me$_2$TFA*), 46.3 (CH$_3$ of Me$_2$TFA*), 52.7 (CMe$_2$ of TMP), 66.7 (CH**C**H$_2$NMe$_2$ of Me$_2$TFA*), 76.1 (**C**HCH$_2$NMe$_2$ of Me$_2$TFA*), 84.3 (AlCH of Me$_2$TFA*).

Diastereomer B: δ_C (100.62 MHz, THF-D$_8$, 298 K) 19.6 (γCH$_2$ of TMP), 28.2 (CH of ^{i}Bu), 28.3 (CH of ^{i}Bu), 33.0 (AlCH**C**H$_2$ of Me$_2$TFA*), 34.4 (CH$_3$ of TMP), 34.6 (CH$_3$ of TMP), 44.2 (AlCH**C**H$_2$ of Me$_2$TFA*), 46.1 (CH$_3$ of Me$_2$TFA*), 52.5 (CMe$_2$ of TMP), 65.8 (CH**C**H$_2$NMe$_2$ of Me$_2$TFA*), 76.5 (**C**HCH$_2$NMe$_2$ of Me$_2$TFA*), 84.5 (AlCH of Me$_2$TFA*).

Diastereomer A/B δ_C (100.62 MHz, THF-D$_8$, 298 K) 30.4 (CH$_2$ of ^{i}Bu), 29.9 (CH$_2$ of ^{i}Bu), 29.0 (CH$_2$ of ^{i}Bu), 28.7 (CH$_2$ of ^{i}Bu). Due to a complex ^{1}H NMR spectrum the CH$_3$ of ^{i}Bu and βCH$_2$ of TMP could only be assigned to 29.4, 29.7, 30.1, and 31.2 ppm and could not be differentiated.

δ_{Li} (155.50 MHz, THF-D$_8$, 298 K) 0.33.

Synthesis of [Me$_2$TFA·Li(μ-TMP)(μ-^{i}Bu)Al(^{i}Bu)$_2$] **2C**

Hexane (10 mL) was introduced to an oven-dried Schlenk tube. Next, 1.6 M *n*BuLi (1.25 mL, 2 mmol) was added, followed by TMP(H) (0.34 mL, 2 mmol) at room temperature. The reaction mixture was left to stir for 10 min and then ^{i}Bu$_3$Al (2 mL, 2 mmol) was injected into it. Finally, Me$_2$TFA (0.28 mL, 2 mmol) was added and the reaction mixture was left to stir overnight. The solution was left to stand at −30°C. A crop of colourless crystals formed (0.58 g, 61 %) in solution, which were successfully studied by X-ray crystallographic analysis.

δ_H (400.13 MHz, THF-D$_8$, 298 K) −0.34 (1H, m, CH$_2$ of ^{i}Bu), −0.20 (5H, d, ^3J(H, H) 6.3, CH$_2$ of ^{i}Bu), 0.84 (15H, d, ^3J(H, H) 6.4, CH$_3$ of ^{i}Bu), 0.89 (3H, d, ^3J(H, H) 6.4, CH$_3$ of ^{i}Bu), 1.22 (4H, m, βCH$_2$ of TMP), 1.22 (12H, s, CH$_3$ of TMP), 1.52 (2H, m, γCH$_2$ of TMP), 1.54 (1H, m, OCHC*H*$_2$ of Me$_2$TFA), 1.81 (2H, m, OCH$_2$C*H*$_2$ of Me$_2$TFA), 1.89 (3H, m, CH of ^{i}Bu), 1.93 (1H, m, OCHC*H*$_2$ of Me$_2$TFA), 2.20 (6H, s, NC*H*$_3$ of Me$_2$TFA), 2.30 (2H, m, C*H*$_2$NMe$_2$ of Me$_2$TFA), 3.64 (1H, m, αC*H*$_2$ of Me$_2$TFA), 3.78 (1H, m, αCH$_2$ of Me$_2$TFA), 3.90 ppm (1H, m, αCH of Me$_2$TFA).

δ_C (100.62 MHz, THF-D$_8$, 298 K) 20.2 (γCH$_2$ of TMP), 26.2 (OCH$_2$**C**H$_2$ of Me$_2$TFA), 30.0 (CH$_2$ of ^{i}Bu), 28.7 (CH of ^{i}Bu), 30.2 (CH$_3$ of ^{i}Bu), 30.8 (OCH**C**H$_2$ of Me$_2$TFA), 34.6 (Me of TMP), 45.3 (βCH$_2$ of TMP), 46.5 (NMe$_2$ of Me$_2$TFA), 52.5 (CMe$_2$ of TMP), 64.8 (CH$_2$NMe$_2$ of Me$_2$TFA), 68.4 (OCH$_2$ of Me$_2$TFA), 78.7 (OCH of Me$_2$TFA).

δ_{Li} (155.50 MHz, THF-D$_8$, 298 K) −0.43.

Synthesis of [Li(μ-TMP)(μ-MDAE)Al(^{i}Bu)$_2$]* **1D**

This was prepared as per complex **1C** but with MDAE (0.25 mL, 2 mmol) injected to the in situ generated lithium aluminate base. The solution was left to stand in the freezer at −30°C. A crop of colourless crystals (0.63 g, 81 %) formed in solution, which were successfully studied by X-ray crystallographic analysis.

δ_H (400.13 MHz, THF-D$_8$, 298 K) −0.12 (4H, m, CH$_2$ of ^{i}Bu), 0.88 (6H, d, ^3J(H, H) 6.4, CH$_3$ of ^{i}Bu), 0.90 (6H, d, ^3J(H, H) 6.4, CH$_3$ of ^{i}Bu), 1.25 (4H, m, βCH$_2$ of TMP), 1.25 (12H, s, CH$_3$ of TMP), 1.59 (2H, m, γCH$_2$ of TMP), 1.86 (2H, m, CH of ^{i}Bu), 2.26 (6H, s, NMe$_2$ of MDAE*), 2.46 (2H, m, Me$_2$NCH$_2$ of MDAE*), 3.20 (2H, s, AlCH$_2$ of MDAE*), 3.57 (2H, m, AlCH$_2$OC*H*$_2$ of MDAE*).

δ_C (100.62 MHz, THF-D$_8$, 298 K) 19.6 (γCH$_2$ of TMP), 28.3 (CH of ^{i}Bu), 29.2 (CH$_3$ of ^{i}Bu), 30.0 (CH$_3$ of ^{i}Bu), 30.8 (CH$_2$ of ^{i}Bu), 33.9 (CH$_3$ of TMP), 45.0 (βCH$_2$ of TMP), 45.5 (NMe$_2$ of MDAE*), 52.6 (CMe$_2$ of TMP), 60.0 (Me$_2$NCH$_2$ of MDAE*), 71.7 (AlCH$_2$O**C**H$_2$ of MDAE*), 78.0 (AlCH$_2$ of MDAE*).

δ_{Li} (155.50 MHz, THF-D$_8$, 298 K) 0.19.

Synthesis of [MDAE·Li(μ-TMP)(μ-^{i}Bu)Al(^{i}Bu)$_2$] **2D**

This was prepared as per complex **2C** but with MDAE (0.25 mL, 2 mmol) injected to the in situ generated lithium aluminate base. The solution was left to stand in the freezer at −30°C. A crop of colourless crystals (0.30 g, 33 %) formed in solution, which were successfully studied by X-ray crystallographic analysis.

δ_H (400.13 MHz, 298 K, C$_6$D$_6$) 0.27 (6H, d, ^3J(H, H) 6.50, 3 × CH$_2$ of ^{i}Bu), 1.40 (2H, m, 1 × βCH$_2$ of TMP), 1.42 (15H, d, ^3J(H, H) 6.50, 5 × CH$_3$ of ^{i}Bu), 1.46 (3H, d, ^3J(H, H) 6.50, 1 × CH$_3$ of ^{i}Bu), 1.50 (12H, broad s, 4 × CH$_3$ of TMP), 1.70 (6H, s, N(CH$_3$)$_2$ of MDAE), 1.76 (2H, t, ^3J(H, H) 5.18, NCH$_2$ of MDAE), 2.43 (3H, m, 3 × CH of ^{i}Bu), 2.64 (2H, s, OCH$_2$ of MDAE), 2.93 (3H, s, OCH$_3$ of MDAE).

δ_C (100.62 MHz, 298 K, C_6D_6) 18.8 (γCH_2 of TMP), 27.7 (CH of ^{i}Bu), 27.8 (βCH_2 of TMP), 28.6 (CH_3 of TMP), 29.4 (CH_3 of TMP), 29.7 (CH_3 of ^{i}Bu), 29.9 (CH_2 of ^{i}Bu), 45.0 (βCH_2 of TMP), 45.1 (NCH_3 of MDAE), 52.8 (CMe_2 of TMP), 57.8 (NCH_2 of MDAE), 59.4 (OCH_3 of MDAE), 68.2 (OCH_2 of MDAE).

δ_{Li} (155.50 MHz, 298 K, C_6D_6) −0.34.

Synthesis of [Li(μ-TMP)(μ-Me$_4$AEE)Al(^{i}Bu)$_2$]* ***1E***

This was prepared as per complex **1C** but with Me_4AEE (0.38 mL, 2 mmol) injected to the in situ generated lithium aluminate base, producing a white precipitate which dissolved on gentle heating. A crop of colourless crystals (0.38 g, 42 %) formed in solution while cooling to room temperature.

δ_H (400.13 MHz, 298 K, C_6D_6) 0.48–0.54 (4H, m, 2 × CH_2 of ^{i}Bu), 1.34 (1H, m, γCH of TMP), 1.36–1.46 (12H, m, 4 × CH_3 of ^{i}Bu), 1.51 (12H, br s, CH_3 of TMP), 1.55 (1H, m, OCH_2CH_2 of Me_4AEE*), 1.60 (6H, s, $N(CH_3)_2$ of Me_4AEE*), 1.84 (1H, m, γCH of TMP), 2.02 (1H, m, OCH_2CH_2 of Me_4AEE*), 2.25 (6H, s, $N(CH_3)_2$ of Me_4AEE*), 2.35 (2H, m, 2 × CH of ^{i}Bu), 2.66 (1H, d, ^3J(H, H) 14.4, $OCHCH_2$ of Me_4AEE*), 3.15 (1H, m, OCH_2 of Me_4AEE*), 3.28 (1H, m, OCH of Me_4AEE*), 3.50 (1H, d, ^3J(H, H) 11.1Hz, $OCHCH_2$ of Me_4AEE*), 4.48 (1H, m, OCH_2 of Me_4AEE*).

δ_C (100.62 MHz, 298 K, C_6D_6) 18.3 (γCH_2 of TMP), 27.6 (CH of ^{i}Bu), 27.8 (CH of ^{i}Bu), 29.0 (CH_2 of ^{i}Bu), 28.6 (CH_3 of ^{i}Bu), 29.4 (CH_3 of ^{i}Bu), 29.6 (CH_3 of ^{i}Bu), 35.7 (CH_3 of TMP), 30.2 (CH_3 of ^{i}Bu), 43.2 (CH_3 of Me_4AEE*), 45.4 (CH_3 of Me_4AEE*), 46.1 (CH_3 of Me_4AEE*), 60.1 ($OCH_2\mathbf{C}H_2$ of Me_4AEE*), 68.2 ($OCH\mathbf{C}H_2$ of Me_4AEE*), 69.7 (OCH_2 of Me_4AEE*), 82.0 (OCH of Me_4AEE).

δ_{Li} (155.50 MHz, 298K, C_6D_6) 1.34.

Synthesis of DME·[Li(μ-TMP)(μ-DME)Al(^{i}Bu)$_2$]$_2$* ***1F***

This was prepared as per complex **1C** but with DME (0.21 mL, 2 mmol) injected to the in situ generated lithium aluminate base, producing a white precipitate which dissolved on gentle heating. A crop of colourless crystals (0.45 g, 64 %) formed in solution while cooling to room temperature.

δ_H (400.13 MHz, C_6D_6, 298 K) 0.42–0.70 (8H, m, 4 × CH_2 of ^{i}Bu), 1.09 (8H, br t, 2 × βCH_2 of TMP), 1.35 (12H, d, ^3J(H, H) 6.4, 4 × CH_3 of ^{i}Bu), 1.41 (12H, d, ^3J(H, H) 6.4, 4 × CH_3 of ^{i}Bu), 1.42 (24H, s, 8 × CH_3 of TMP), 1.56 (4H, m, γCH_2 of TMP), 2.32 (4H, sept, ^3J(H, H) 6.4, 4 × CH of ^{i}Bu), 2.58 (6H, s, 2 × CH_3 of DME*), 2.61 (4H, t, ^3J(H, H) 5.0, OCH_2 of DME*), 2.95 (4H, t, ^3J(H, H) 5.0, OCH_2 of DME*), 3.00 (6H, s, CH_3 of DME), 3.03 (4H, s, CH_2^- of DME*), 3.37 (4H, s, OCH_2 of DME).

δ_{Li} (155.50 MHz, C_6D_6, 298 K) 0.77.

When left to stir for 24 h, a second crystalline material was also deposited in a low yield along with **1F** (DME·Li(μ-TMP)(μ-OMe)Al(^{i}Bu)$_2$, **1FA**). This material could not be isolated in pure form for NMR spectroscopic analysis.

Synthesis of [DME·Li(μ-TMP)(μ-^{i}Bu)Al(^{i}Bu)$_2$] ***2F***

This was prepared as per complex **2C** but with DME (0.21 mL, 2 mmol) injected to the in situ generated lithium aluminate base. The Schlenk tube was left to stand at 0°C where a crop of colourless crystals (0.42 g, 48 %) formed in solution, which were successfully studied by X-ray crystallographic analysis.

δ_H (400.13 MHz, C_6D_6, 298 K) 0.21 (1H, m, CH_2 of ^{i}Bu), 0.29 (5H, d, ^3J(H, H) 6.1, CH_2 of ^{i}Bu), 1.40 (18H, d, ^3J(H, H) 6.6, CH_3 of ^{i}Bu), 1.52 (12H, br s, CH_3 of TMP), 2.40 (3H, m, CH of ^{i}Bu), 2.68 (4H, s, CH_2 of DME), 2.86 (6H, s, CH_3 of DME).

δ_C (100.62 MHz, C_6D_6, 298 K) 18.9 (γCH_2 of TMP), 27.8 (CH_3 of ^{i}Bu), 27.8 (CH of ^{i}Bu), 29.7 (CH_3 of TMP), 44.8 (βCH_2 of TMP), 52.8 (CMe_2 of TMP), 59.0 (CH_3 of DME), 69.7 (CH_2 of DME).

δ_{Li} (155.50 MHz, C_6D_6, 298 K) −0.45.

Synthesis of [Li(Me$_2$NC$_6$H$_{10}$NMeCH$_2$)$_2$Al(^{i}Bu)$_2$] ***2H***

This aluminate was prepared analogously to complex **2C** but with TMCDA (0.38 mL, 2 mmol) injected to the in situ generated lithium aluminate base. The Schlenk tube was left in the freezer at −30°C. A crop of colourless crystals (0.27 g, 28 %) formed in solution that were suitable for X-ray crystallographic analysis. The rational synthesis of **2H** was attempted using two molar equivalents of the Lewis base (0.76 mL, 4 mmol of TMCDA), however, an oil formed in solution and no crystals could be grown.

Attempts to prepare **1G**, **1H**, **2E**, and **2G** were made by combining the appropriate lithium aluminate base and donor, however, in each case no tangible products were obtained.

Synthesis of [Me$_2$NCH$_2$CH$_2$OCH (C$_6$H$_4$OCH$_3$)CH$_2$NMe$_2$] ***3E***

Compound **1E** was synthesised on a 2 mmol scale as described above. Hexane was removed under vacuum and 10 mL of dry THF was added. Four molar equivalents of $Zn(OAc)_2$ (8 mmol, 1.48 g) was added and the mixture allowed to stir overnight. In a separate Schlenk tube 2 mol-% (0.009 g) of $Pd(OAc)_2$ was added together with 4 mol-% (0.03 g) of 2-dicyclohexylphosphino-2′,6′-dimethoxybiphenyl to give $Pd(OAc)_2$/SPhos. THF (5 mL) was added and the solution was allowed to stir until the solid had completely dissolved. Three equivalents of 4-iodoanisole was added and this solution was added to the first solution through a cannula. This combined solution was left to stir overnight. A saturated solution of ammonium chloride (20 mL) was added and the organic layer was separated from the aqueous layer, washing twice with ethyl acetate. Ammonia solution and ethyl acetate were added to the aqueous layer and the organic layer was once again separated from the aqueous layer. The organic layer was concentrated under vacuum to leave **3E** and TMP(H) as a crude product. The TMP(H) was removed under vacuum to give **3E** in 62 % (0.27 g) yield.

δ_H (400.13 MHz, $CDCl_3$, 298 K) 2.23 (6H, s, $N\{CH_3\}_2$), 2.31 (6H, s, $N\{CH_3\}_2$), 2.29 (1H, m, CH of CH_2), 2.43 (1H, m, CH of CH_2), 2.55 (1H, m, CH of CH_2), 2.76 (1H, m, CH of CH_2), 3.35 (2H, m, CH_2), 3.79 (3H, s, OCH_3), 4.38 (1H, dd, ^3J(H, H) 9.04, 3.51, CH next to O), 6.86 (2H, d, ^3J(H, H) 8.7, 2 × CH aromatic), 7.22 ppm (2H, d, ^3J(H, H) 8.7, 2 × CH aromatic).

δ_C (100.62 MHz, $CDCl_3$, 298 K) 45.5 ($N\{CH_3\}_2$), 45.8 ($N\{CH_3\}_2$), 55.2 (OCH_3), 59.0 (CH_2), 65.9 (CH_2), 66.4 (CH_2), 79.9 (CH next to O), 113.9 (2 × CH of aromatic), 127.9 (2 × CH of aromatic), 133.9 (quaternary *para* C of aromatic), 159.2 (quaternary C of aromatic next to OMe).

Deuterium Studies

One millilitre of D_2O was added by syringe to an in situ generated solution of complexes **1** and **2** and this was allowed to stir for 15 min. This was then dried with $MgSO_3$, filtered, and concentrated under vacuum. The resulting mixtures were analysed for deuterium uptake by ^{2}D NMR spectroscopy in $CHCl_3$ (see Table 1), with the resulting spectra referenced to the solvent.

Crystallographic Analysis

Crystallographic data was collected at 123(2) K on Oxford Diffraction instruments with $Mo_{K\alpha}$ (λ 0.71073 Å) radiation. Structures were solved using the *SHELXS-97* program[35] and were refined to convergence against F^2 against all independent reflections by the full-matrix least-squares method using the *SHELXL-97* program.[35] The quality of the structure of **1C** was adversely affected by disorder in the deprotonated Me_2TFA ligand. Selected crystallographic and refinement parameters are given in Table S1. CCDC 932147–932153 contain the supplementary crystallographic data for this paper. These data can be obtained free of charge from The Cambridge Crystallographic Data Centre via www.ccdc.cam.ac.uk/data_request/cif.

Results and Discussion

Solid State Studies

The experimental protocol followed was simply to stir the lithium aluminate bases **1** or **2** in hexane solution in the presence of an equimolar quantity of each of the six neutral Lewis base molecules (**C**–**H**) displayed in Fig. 1. Of the twelve potential organometallic products, seven were prepared in crystalline form suitable for single crystal X-ray diffraction analysis. The molecular structure results of these analyses are displayed in Figs 2–8. What is instantly clear is, mirroring the THF examples shown in Scheme 1a, the fully intact donor molecules simply coordinate datively to base **2** (this could be regarded as 'co-complexation'), contributing to the four-coordinate, distorted tetrahedral lithium environments shown in Figs 5–7. In marked contrast the di-TMP base **1** C–H deprotonates all of the involved donors by TMP basicity to complete three-coordinate lithium centres and five-membered Li–N–Al–C–O

Table 1. Deuterium NMR studies on in situ prepared bases

In situ prepared base	^{2}D NMR(δ)	Assignment
1C	3.85, 3.71	OCH*D*, OC*D*H
2C	3.85, 3.71, 2.26	OCH*D*, OC*D*H, NCH_2D
1D	3.41	OCH_2D
2D	–	–
1E	3.53, 2.26	OCH*D*, NCH_2D
2E	–	–
1F	3.38	OCH_2D
2F	–	–
1G	2.26	NCH_2D
2G	–	–
1H	2.29	NCH_2D
2H	2.29	NCH_2D

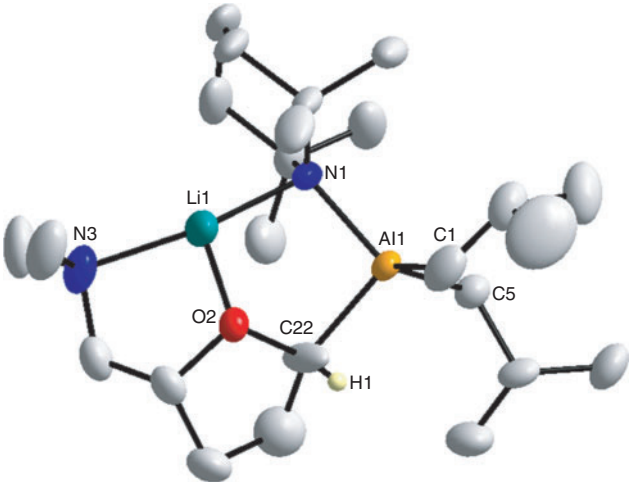

Fig. 2. Molecular structure of α-deprotonated *N*,*N*-dimethyltetrahydrofurfurylamine (Me_2TFA) compound **1C** [Li(μ-$Me_2NCH_2CHCH_2CH_2CHO$)(μ-TMP)Al(^{t}Bu)$_2$]. Ellipsoids are drawn at 50 % probability level and hydrogen atoms, except that on the metallated carbon, are omitted for clarity. The Me_2TFA and one ^{t}Bu group were modelled as disordered in a 76 : 24 and 51 : 49 ratio respectively, only the major components are displayed for clarity.

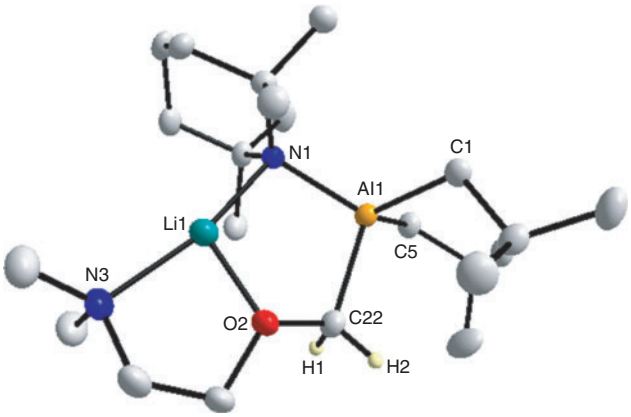

Fig. 3. Molecular structure of deprotonated 1-methoxy-2-dimethylaminoethane (MDAE) compound **1D** [Li(μ-$Me_2NCH_2CH_2OCH_2$)(μ-TMP)Al(^{t}Bu)$_2$]. Ellipsoids are drawn at 50 % probability level and hydrogen atoms, except those on the metallated carbon, are omitted for clarity.

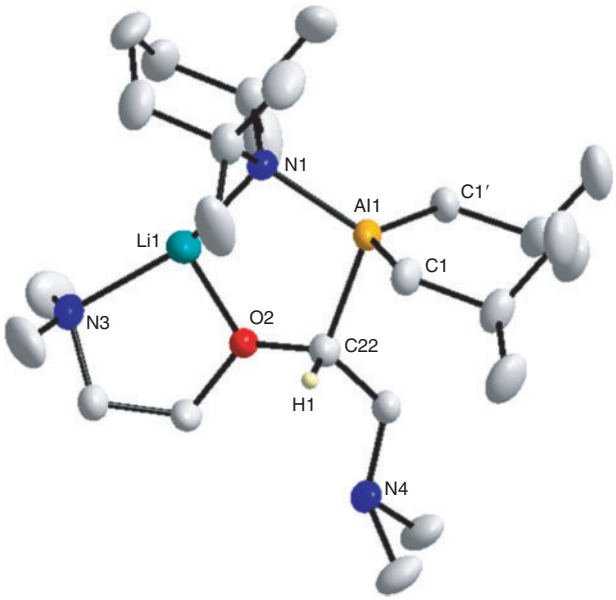

Fig. 4. Molecular structure of deprotonated bis[2-(*N*,*N*-dimethylamino)ethyl]ether (Me_4AEE) compound **1E** [Li(μ-$Me_2NCH_2CH_2OCHCH_2NMe_2$)(μ-TMP)Al(^{t}Bu)$_2$]. Ellipsoids are drawn at 50 % probability level and hydrogen atoms, except that on the metallated carbon, are omitted for clarity. Me_4AEE and ^{t}Bu groups were modelled as disordered in a 50 : 50 ratio. Only one component is shown for clarity.

rings (Figs 2–4 for **1C**, **1D**, and **1E**, respectively). The one exception to this trend is seen in the reaction of base **2** with TMCDA (**2H**, Fig. 8) because two molecules of this chiral donor are deprotonated by dual ^{i}Bu/TMP basicity. Such a scenario has been witnessed before using the similar but achiral bidentate *N*,*N*-donor TMEDA (Scheme 1b) and therefore the arguments presented previously for TMEDA are applicable also to this case.

As shown in Figs 2–4, base **1** preferentially deprotonates (aluminates) selectively at the carbon atom adjacent to oxygen rather than nitrogen when given the choice of either position. With the potentially tridentate *N*,*O*,*N*-donor Me_4AEE (isoelectronic to the common tridentate *N*,*N*,*N*-donor PMDETA, *N*,*N*,*N*′,*N*″,*N*″-pentamethyldiethylenetriamine), deprotonation occurs selectively on one of the methylene groups adjacent to oxygen rather than at a terminal methyl arm, with the ligand then coordinating to lithium in a hypodentate *N*,*O* fashion leaving one CH_2NMe_2 limb uncoordinated and swinging free (Fig. 4).

The three aluminates [Li(μ-$Me_2NCH_2CHCH_2CH_2CHO$)(μ-TMP)Al(^{i}Bu)$_2$] **1C**, [Li(μ-$Me_2NCH_2CH_2OCH_2$)(μ-TMP)Al(^{i}Bu)$_2$] **1D**, and [Li(μ-$Me_2NCH_2CH_2OCHCH_2NMe_2$)

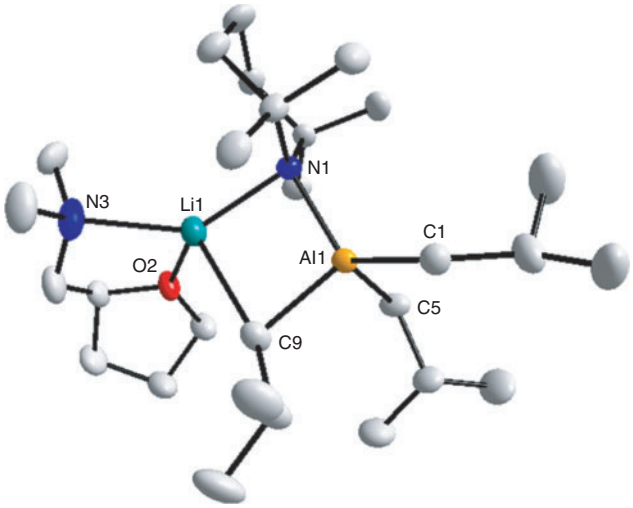

Fig. 5. Molecular structure of solvated *N*,*N*-dimethyltetrahydrofurfurylamine (Me_2TFA) compound **2C** [Me_2TFA·Li(μ-^{i}Bu)(μ-TMP)Al(^{i}Bu)$_2$]. Ellipsoids are drawn at 50 % probability level and hydrogen atoms are omitted for clarity. Part of the Me_2TFA molecule was modelled as disordered in an 88 : 12 ratio. Only the major component is displayed for clarity.

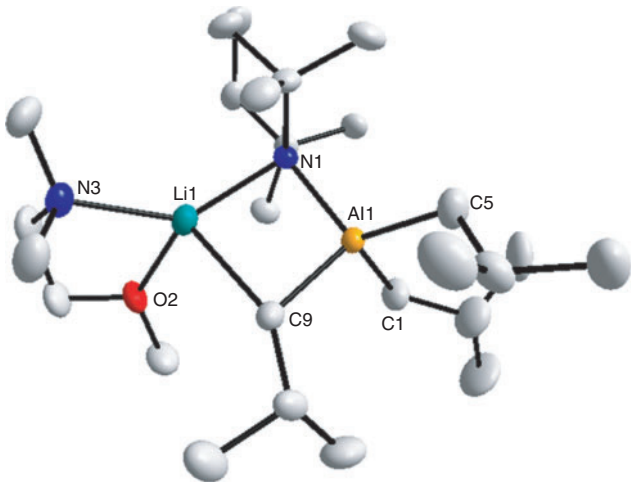

Fig. 6. Molecular structure of solvated 1-methoxy-2-dimethylaminoethane (MDAE) compound **2D** [MDAE·Li(μ-^{i}Bu)(μ-TMP)Al(^{i}Bu)$_2$]. Ellipsoids are drawn at 50 % probability level and hydrogen atoms are omitted for clarity. The crystal structure contained two independent molecules, only one is displayed for clarity.

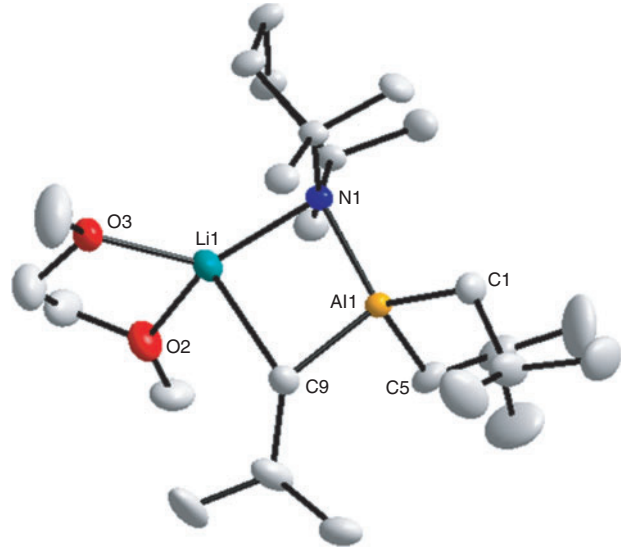

Fig. 7. Molecular structure of solvated 1,2-dimethoxyethane (DME) compound **2F** [DME·Li(μ-^{i}Bu)(μ-TMP)Al(^{i}Bu)$_2$]. Ellipsoids are drawn at 50 % probability level and hydrogen atoms are omitted for clarity.

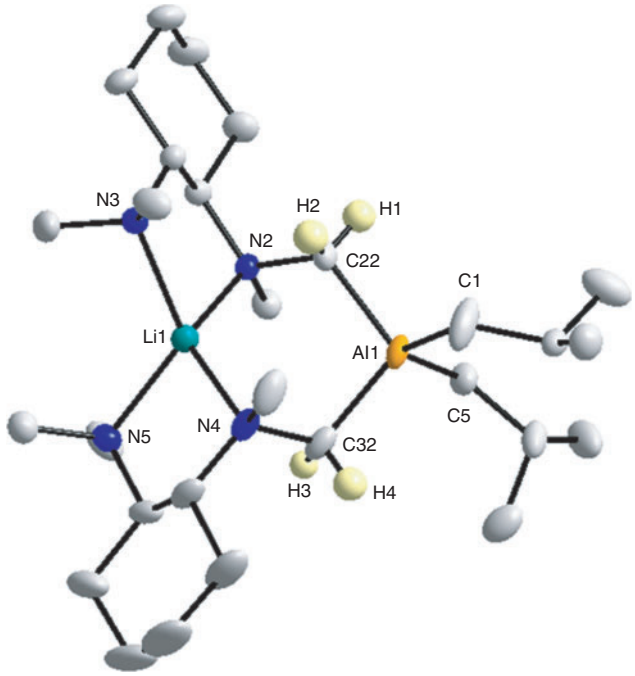

Fig. 8. Molecular structure of deprotoaluminated bis-*N*,*N*,*N*′,*N*′-tetramethylcyclohexanediamine (TMCDA) compound **2H** [Li(μ-$CH_2NMeC_6H_{10}NMe_2$)$_2$Al(^{i}Bu)$_2$]. Ellipsoids are drawn at 50 % probability level and hydrogen atoms, except those on metallated carbon atoms, are omitted for clarity.

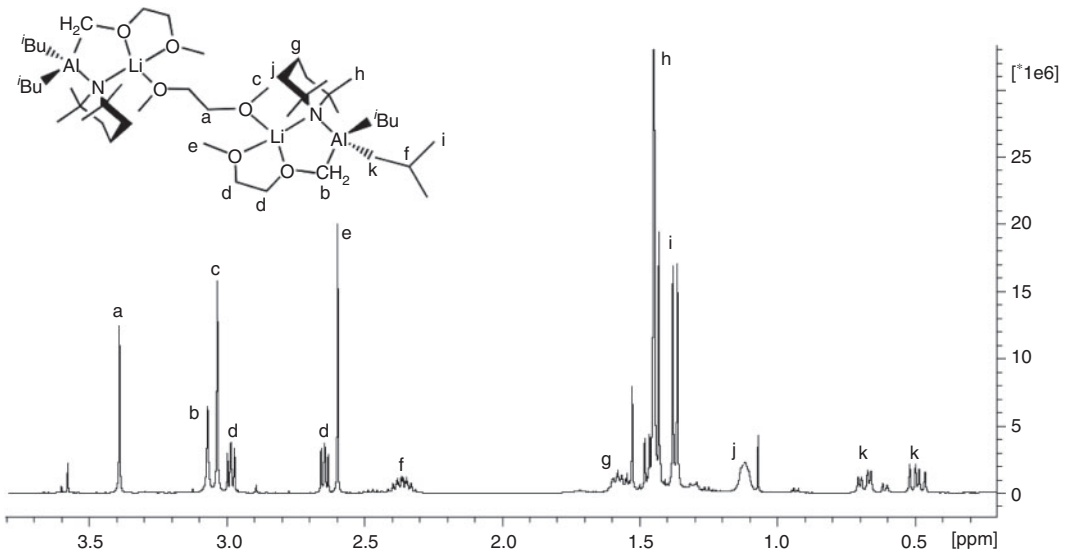

Fig. 9. ^{1}H NMR spectrum of crystalline material from the reaction of base **1** with 1,2-dimethoxyethane (DME) showing full assignment.

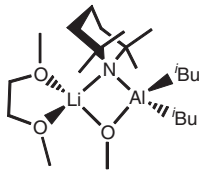

Fig. 10. Proposed structure of cleaved 1,2-dimethoxyethane (DME) product **1FA**.

(μ-TMP)Al(^{i}Bu)$_2$] **1E** with the mono-deprotonated donor ligands are made up of two terminal ^{i}Bu groups on Al, resulting in a distorted tetrahedral geometry, with one TMP bridging Li and Al. The donor ligands are deprotonated in an intramolecular fashion at the most acidic C–H site adjacent to the O atom after prior coordination to Li. The ligand forms the second bridging anion and as a result the deprotonated C and adjacent O complete the central five-element five-membered Al–N–Li–O–C ring. In addition to this multi-element ring, each structure is made up of another one or two rings fused onto the central ring. Compounds **1D** and **1E** are made up of an additional four-element five-membered N–Li–O–C–C ring, the only major difference between these structures is the pendant CH_2NMe_2 arm attached to the deprotonated C of compound **1E**. Aluminate **1C** has two additional fused rings due to the cyclic substituted-THF component of the ligand and NMe_2 dative coordination to Li from the pendant arm which forms an additional four-element five-membered N–Li–O–C–C ring.

Compound **2H** [Li(μ-$CH_2NMeC_6H_{10}NMe_2$)$_2$Al(^{i}Bu)$_2$] differs only in the replacement of the bridging TMP anion with another deprotonated TMCDA ligand which now occupies the bridging site. The compound contains a central four-element six-membered N–C–Al–C–N–Li ring with two fused three-element five-membered N–C–C–N–Li rings while solvated lithium compounds [Me_2TFA·Li(μ-^{i}Bu)(μ-TMP)Al(^{i}Bu)$_2$] **2C**, [MDAE·Li(μ-^{i}Bu)(μ-TMP)Al(^{i}Bu)$_2$] **2D**, and [DME·Li(μ-^{i}Bu)(μ-TMP)Al(^{i}Bu)$_2$] **2F** adopt a similar motif to compounds **1C**, **1D**, and **1E**, however, this time the second bridging anion is an isobutyl ligand rather than a deprotonated donor molecule and the donor ligand with all its hydrogen atoms attached simply solvates the now spirocyclic Li atom. The lack of deprotonation of these chelating donor ligands is further backed up by the ^{1}H NMR spectroscopic data which confirms the presence of an intact donor ligand.

A crystalline product was also obtained from the reaction in hexane of bis-TMP base **1** with the bis-oxygen donor molecule DME; however, crystals of **1F** proved not to be of X-ray quality precluding us from obtaining a suitable X-ray crystal structure. However, the ^{1}H NMR spectrum of **1F** in C_6D_6 (Fig. 9) shows that deprotonation at one terminal methyl group has occurred as two triplets are observed at 2.61 and 2.95 ppm resulting from loss of symmetry of the CH_2–CH_2 backbone. The signals for the two terminal Al-bound isobutyl groups can be seen as a multiplet at 0.42–0.70 ppm for the CH_2 protons, two doublets at 1.35 and 1.41 ppm for the CH_3 protons, and a septet at 2.32 ppm for the CH protons. TMP methyl protons can be seen at 1.42 ppm. The integration of the two singlets at 2.58 and 3.03 ppm are consistent with the methyl and CH_2 hydrogen atoms of a methyl deprotonated DME ligand. The two remaining singlets at 3.00 and 3.37 ppm are consistent with the CH_3 and CH_2 hydrogen atoms of a second, fully intact DME molecule. The integration of the intact DME against the deprotonated DME indicates a 1 : 2 ratio. As these signals are shifted compared with free DME (methyl, 3.40; methylene, 3.55 ppm) it can be proposed that the structure might contain one donor DME bridging two typical deprotonated motifs to give [(^{i}Bu)$_2$Al(μ-TMP)(μ-$CH_3OCH_2CH_2OCH_2$)Li(DME)Li(μ-$CH_2OCH_2CH_2OCH_3$)(μ-TMP)Al(^{i}Bu)$_2$] (Fig. 9, inset). Such a structure clearly has similarities with the lithium aluminate dioxan complex (see above) which also contains a neutral molecule acting as a bridging ligand with deprotonated versions of the same ligand bridging between lithium and aluminium.

When a solution of **1** containing DME was allowed to stir for longer (24 h) a second product in addition to **1F** was found to co-crystallise within the solution. The ^{1}H NMR spectrum shows a mixture of the proposed compound shown above (**1F**) and a second product **1FA**. The X-ray crystal data of **1FA** is of insufficient quality to discuss in any detail, however, these data

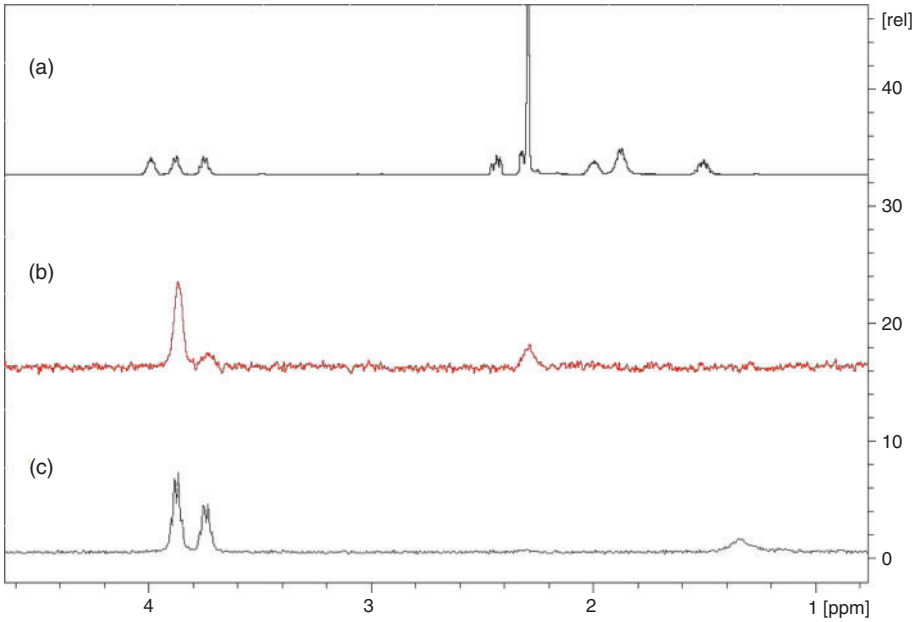

Fig. 11. (a) ^{1}H NMR spectrum of free *N*,*N*-dimethyltetrahydrofurfurylamine (Me_2TFA), (b) ^{2}D NMR spectra for the deuterium quench of Me_2TFA after reaction with base **2** or (c) base **1**.

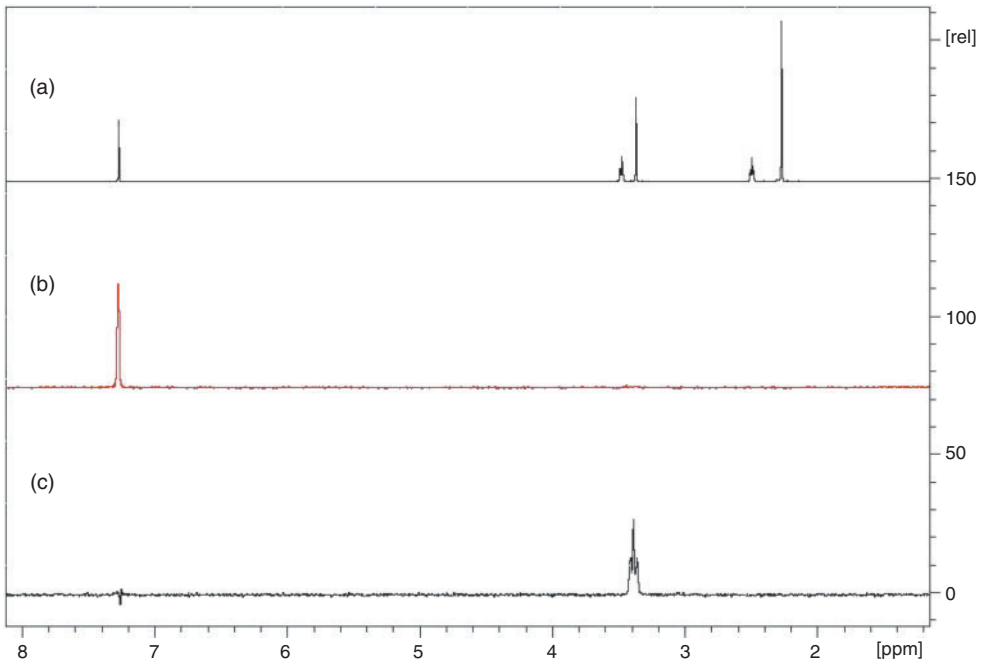

Fig. 12. (a) ^{1}H NMR spectrum of free 1-methoxy-2-dimethylaminoethane (MDAE), (b) ^{2}D NMR spectra for the deuterium quench of MDAE after reaction with base **2** or (c) base **1**.

suggest that the product contains a trapped OMe group in the bridging position between Li and Al and a fully intact donor DME on Li instead of a deprotonated diether DME giving DME·Li(μ-TMP)(μ-OMe)Al(^{i}Bu)$_2$ (Fig. 10). This suggests that after time the deprotonated DME[36–39] cleaves at the MeO–CH_2 junction with the resulting methoxy group subsequently becoming trapped, although the mechanism through which this occurs is unclear.[40] Reactions of this type have been discussed in terms of 'cleave and capture chemistry' as recently described in a perspective article.[41]

Solution State Studies

A solution state NMR spectroscopic study was initiated on the highly soluble crystalline material obtained from these reactions (see above). ^{1}H and ^{13}C NMR spectra in C_6D_6 or D_8-THF were consistent with the molecular structures discussed

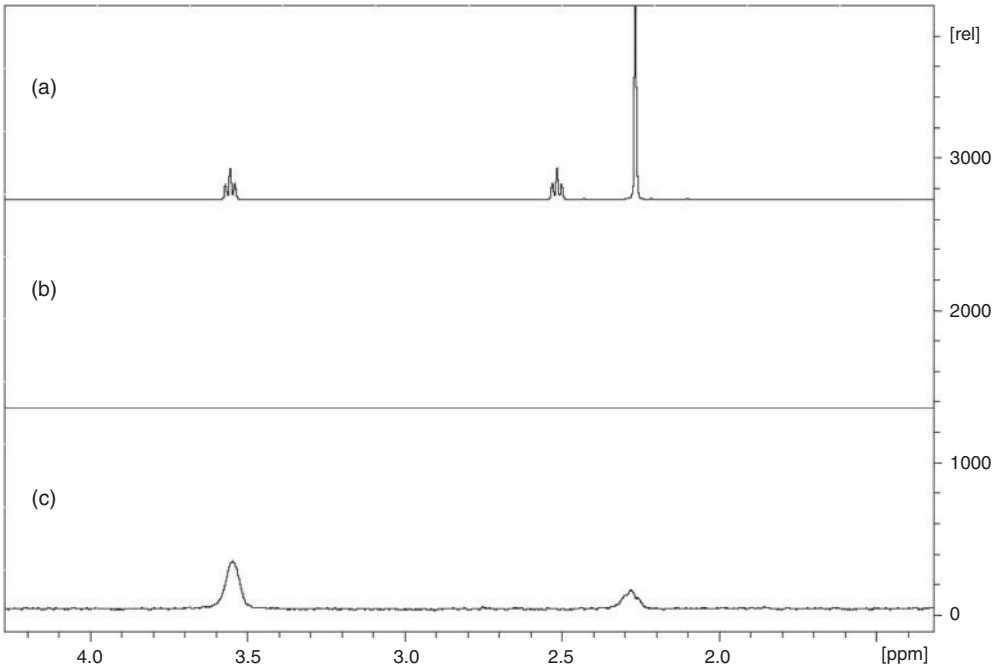

Fig. 13. (a) ^{1}H NMR spectrum of free bis[2-(*N*,*N*-dimethylamino)ethyl]ether (Me_4AEE), (b) ^{2}D NMR spectra for the deuterium quench of Me_4AEE after reaction with base **2** or (c) base **1**.

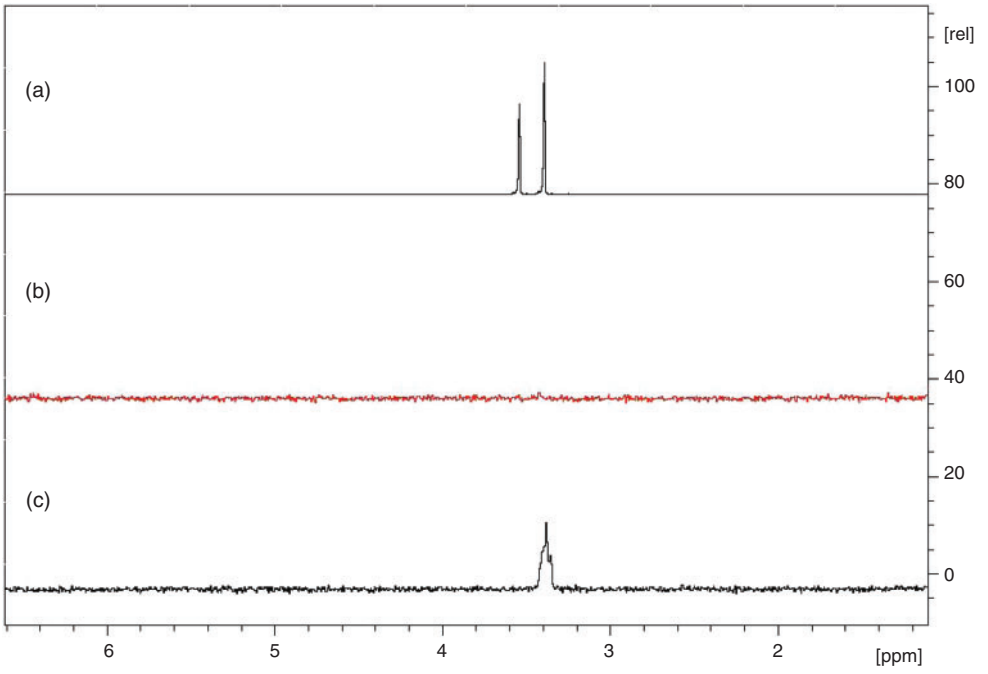

Fig. 14. (a) ^{1}H NMR spectrum of free 1,2-dimethoxyethane (DME), (b) ^{2}D NMR spectra for the deuterium quench of DME after reaction with base **2** or (c) base **1**.

previously, with complexes **1** each displaying a 2 : 1 : 1 ^{i}Bu/TMP/deprotonated-donor ratio and complexes **2** each displaying a 3 : 1 : 1 ^{i}Bu/TMP/intact-donor ratio in their ^{1}H resonance integrations. The one exception to this was found in **2H**, which displays a 1 : 1 ^{i}Bu/deprotonated-TMCDA ratio. In the case of **1C**, resonances representing two diastereomers were witnessed (in a 2 : 1 ratio) as a consequence of deprotonation of the methylene group adjacent to oxygen (C22 in Fig. 2) in the substituted THF ring generating a stereogenic carbon centre. This is noteworthy as no distinction between diastereomers was evident when a chiral carbon centre was generated in **1E** or when THF was the substrate.[23] The most informative resonances

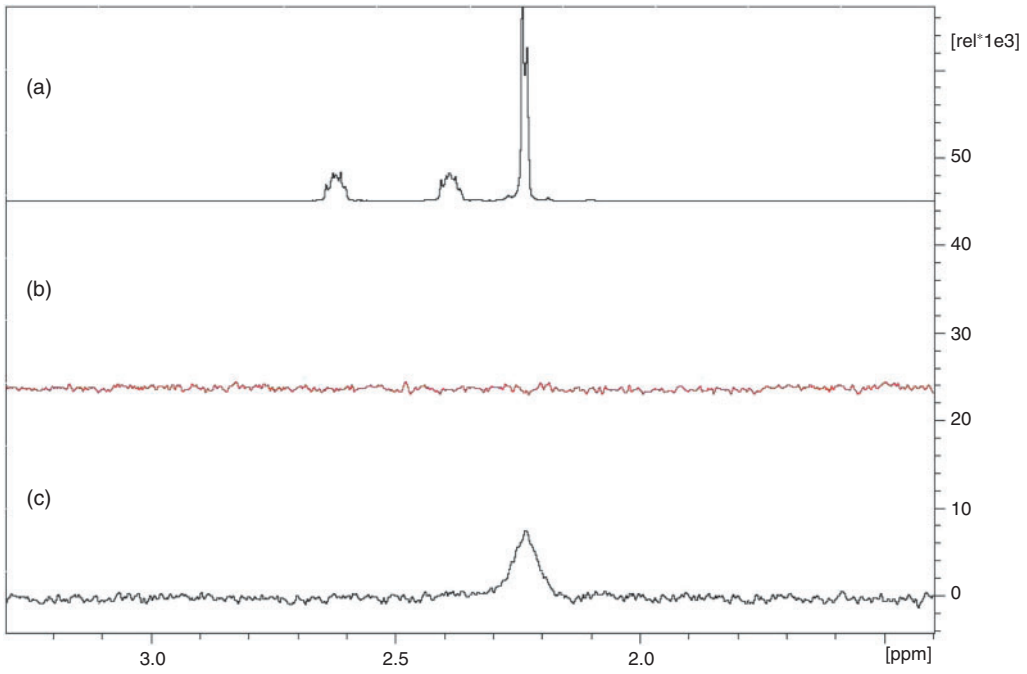

Fig. 15. (a) ^{1}H NMR spectrum of free tris(*N*,*N*-dimethyl-2-aminoethyl)amine (Me_6TREN), (b) ^{2}D NMR spectra for the deuterium quench of Me_6TREN after reaction with base **2** or (c) base **1**.

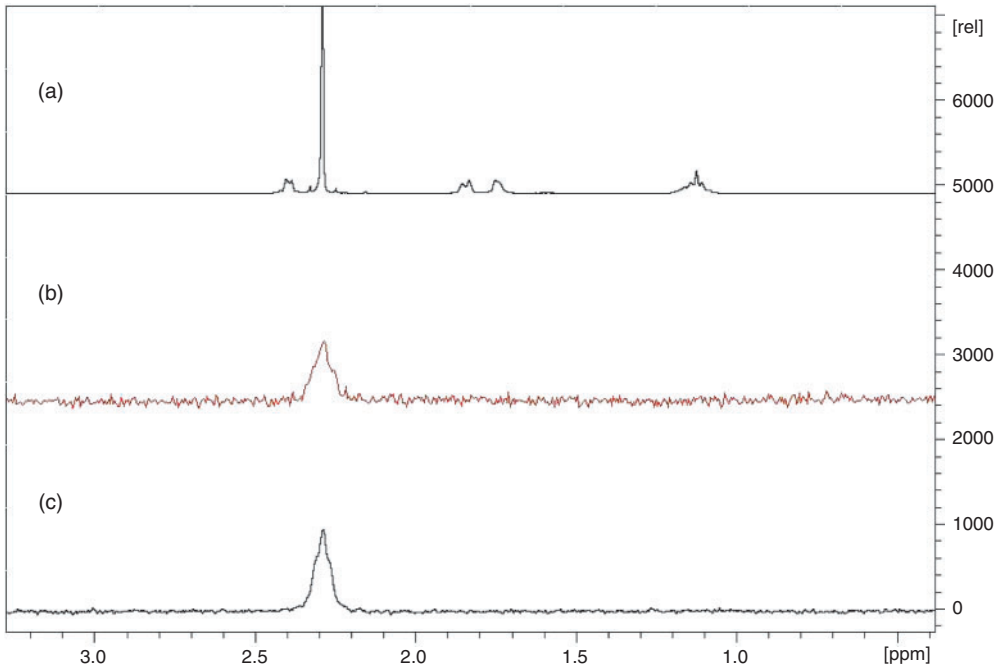

Fig. 16. (a) ^{1}H NMR spectrum of free *R*,*R*,*N*,*N*,*N*′,*N*′-tetramethylcyclohexanediamine (TMCDA), (b) ^{2}D NMR spectra for the deuterium quench of TMCDA after reaction with base **2** or (c) base **1**.

were those of the hydrogen atoms bonded to the metallated carbon atom as well as the metallated carbon atoms themselves. Specifically, resonances at 3.26/3.37 (diastereomer A/B), 3.20, and 3.28 ppm were witnessed in the ^{1}H NMR spectra of complexes **1C**, **1D**, and **1E**, respectively (compare with 3.75/3.86, 3.37, and 3.45 ppm for the corresponding resonances in the free donor ligands). In the ^{13}C NMR spectra, the resonances of the metallated carbon atom were located downfield at 84.3/84.5, 78.0, and 82.0 ppm for **1C**, **1D**, and **1E**, while the non-metallated derivatives **2C** and **2D** showed these carbon resonances at 68.4 and 59.4 ppm, respectively. Meanwhile, the NMR spectra of **2F** suggested no deprotonation of the donor ligand had occurred due

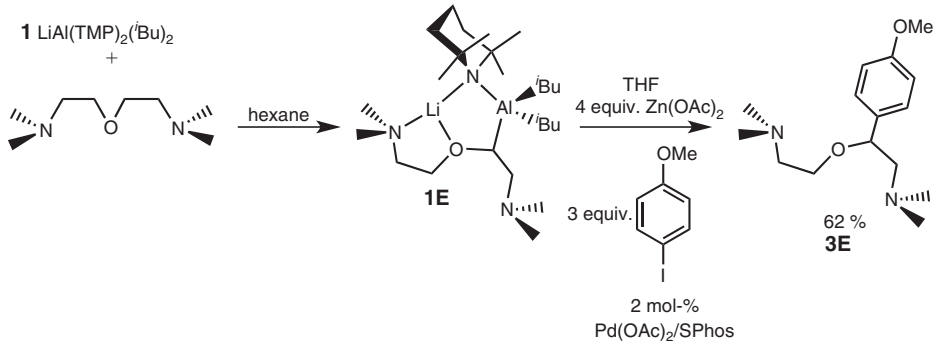

Scheme 3. Deprotonation of bis[2-(*N*,*N*-dimethylamino)ethyl]ether (Me_4AEE) with base **1**, transmetallation with $Zn(OAc)_2$ and subsequent cross-coupling in THF with 2 mol-% $Pd(OAc)_2$/SPhos and three equivalents of 4-iodoanisole to give compound **3E**.

to the resonances indicating its symmetrical chemical makeup remained. Complex **2H** gave a highly complicated NMR spectrum, in part we believe due to the formation of stereogenic centres, which could not be satisfactorily assigned due to overlap of a forest of peaks.

Aware that the NMR spectrum of a crop of isolated crystals is not necessarily representative of the whole in situ generated reaction mixture from which the crystals grew, we also carried out a series of electrophilic quenches on these mixtures to ascertain if the reactivity of **1** and **2** was consistent towards the other donor molecules. Specifically, a deuterium quench (using D_2O) was carried out with the resulting ^2D NMR spectrum consequently compared with the ^1H spectrum of the parent donors to ascertain whether the base had abstracted a proton from them or not.

The deuterium studies reveal some interesting results which cannot be gleaned from the crystal structures in isolation. A comparison of the ^1H NMR spectrum of Me_2TFA with the ^2D NMR spectra of the product formed after it was reacted with base **2** (giving **2C** in the solid state) and then quenched with D_2O (Fig. 11) shows that some deprotonation at the CH_2 group adjacent to oxygen has indeed occurred. There is also a resonance consistent with some NMe_2 deprotonation after reaction with base **2**. The amount of deprotonation must be negligible as a ^1H NMR spectrum of the filtrate solution after the crystals were removed confirms that the major product in solution is consistent with the crystal structure which contains the donor molecule intact, with no evidence of a deprotonation having taken place. Moving to MDAE, as shown in Fig. 12 the deuterium quench resulted in no ^2D incorporation into the ligand after reaction with base **2** while there was clearly ^2D now present on the OMe arm when the more reactive base **1** was used, consistent with this base deprotonating the bidentate ligand. The ^2D NMR spectrum of **1** with Me_4AEE reveals that a small amount of NMe_2 deprotonation has also occurred in addition to the crystallographically determined deprotonation adjacent to oxygen (Fig. 13). The ^2D NMR spectrum of **1** with DME (Fig. 14) confirms that deprotonation has occurred at the methyl group adjacent to O as observed in the ^1H NMR spectrum of the crystals (Fig. 9).

Although crystal structure determinations were not successfully obtained for the products **1G** and **1H**, the D_2O quench experiment performed upon the in situ mixtures revealed that deprotonation at the methyl NMe_2 sites has occurred to some extent (Figs 15 and 16). However, the ^2D NMR spectra for the reaction of **2E** or **2G** with D_2O confirm that no deuterium incorporation into the organic donor ligands has occurred. Overall, aside from the NMe_2 deprotonation of Me_2TFA and Me_4AEE and the αCH_2-deprotonation of Me_2TFA, the D_2O quenches corroborate that the reaction of base **1** or **2** with each ligand follows the same general trend, stronger base **1** deprotonates the donor ligand; whereas the intact ligand simply solvates lithium in the weaker base **2**.

As a representative example Me_4AEE (**E**) was reacted with a variety of electrophiles to determine whether it was possible to selectively functionalise ligands such as these. The best procedure was found to be cross-coupling deprotonated compound **1E** with 4-iodoanisole using a $Pd(OAc)_2$/SPhos[42] catalyst after transmetallation with zinc acetate [$Zn(OAc)_2$] in THF solution (Scheme 3). Due to the presence of three sp^3 carbanionic carbon centres ($1 \times Me_4AEE$ and $2 \times {}^iBu$) three equivalents of 4-iodoanisole were necessary. The new compound **3E** was synthesised in a 62 % yield. To the best of our knowledge this is the first example of the preparation of **3E**.

Due to the amine nitrogen atoms of Me_4AEE the 4-isobutylanisole by-product could be easily removed from the desired product by working up the solution using ammonium chloride and then removing the organic layer. Ammonia solution and ethyl acetate were then added to the aqueous layer leaving only **3E** and TMP(H) as the crude products in the organic layer. Compound **3E** was purified by removing ethyl acetate and TMP(H) under vacuum then characterising by ^1H and ^{13}C NMR spectroscopy in $CDCl_3$ solution. In future work we will investigate quenching procedures and electrophiles for the functionalisation of deprotonated compounds **1C**, **1D**, and **2H**.

Conclusions

This study has demonstrated that the bis-amide $LiAl(TMP)_2{}^iBu_2$ is a far superior deprotonating agent to the mono-amide analogue $LiAl(TMP){}^iBu_3$ and that the deprotonations achieved can be carried out in hexane solution. The aluminium–hydrogen exchanges take place selectively adjacent to the O centre in the mixed N,O ligand sets. In most cases under the conditions studied the mono-amide does not bring about deprotonation but simply engages in a Lewis acid–Lewis base complex with the polydentate donor molecule. A surprising exception to this pattern is that the chiral diamine TMCDA is deprotonated by the weaker aluminating agent at one methyl arm of an NMe_2 group, while the solution investigation shows that the stronger base does this too. Such deprotonations α to a nitrogen atom are relatively challenging so this points to possible energetically favourable intramolecular processes. Although the relative

deprotonating ability of these synergic lithium–aluminium reagents is made clearer through this study, some uncertainty still remains as to the actual constitutions of these reagents in their own right both in hexane and in THF solution. Detailed solution studies using a battery of NMR techniques, as well as theoretical calculations, will be used in future work to shed light on this issue.

Supplementary Material

^{1}H NMR spectra and table of crystallographic data for complexes **1C**, **1D**, **1E**, **2C**, **2D**, **2F**, and **2H** are available on the Journal's website.

Acknowledgements

This work was generously supported by the UK Engineering and Physical Science Research Council (award no. EP/F063733/1), the Royal Society (Wolfson research merit award to REM), a University of Strathclyde RDF award (REM and SDR), and a Royal Society of Edinburgh/BP Trust Fellowship award (SDR).

References

[1] L. Brandsma, H. D. Verkruijsse, *Preparative Polar Organometallic Chemistry* **1987** (Springer: Berlin).
[2] B. J. Wakefield, *Organolithium Methods* **1988** (Academic Press: London).
[3] M. Schlosser, *Organometallics in Synthesis: A Manual, 2nd ed*. **2002** (Wiley: Chichester).
[4] J. Clayden, *Organolithiums: Selectivity for Synthesis* **2002** (Pergamon, Elsevier Science Ltd.: Oxford).
[5] Z. Rappoport, I. Marek (Eds), *The Chemistry of Organolithium Compounds* **2004** (Wiley: New York, NY).
[6] R. E. Mulvey, *Organometallics* **2006**, *25*, 1060. doi:10.1021/OM0510223
[7] R. E. Mulvey, F. Mongin, M. Uchiyama, Y. Kondo, *Angew. Chem. Int. Ed.* **2007**, *46*, 3802. doi:10.1002/ANIE.200604369
[8] R. E. Mulvey, *Acc. Chem. Res.* **2009**, *42*, 743. doi:10.1021/AR800254Y
[9] For an alternative bimetallic approach to alumination, involving the use of LiCl as the lithium source rather than an organolithium reagent see the following excellent review: B. Haag, M. Mosrin, H. Ila, V. Malakhov, P. Knochel, *Angew. Chem. Int. Ed.* **2011**, *50*, 9794. doi:10.1002/ANIE.201101960
[10] G. Linti, H. Schnöckel, *Coord. Chem. Rev.* **2000**, *206–207*, 285. doi:10.1016/S0010-8545(00)00339-8
[11] M. N. S. Rao, H. W. Roesky, G. Anantharaman, *J. Organomet. Chem.* **2002**, *646*, 4. doi:10.1016/S0022-328X(01)00799-9
[12] H. W. Roesky, S. S. Kumar, *Chem. Commun.* **2005**, 4027. doi:10.1039/B505307B
[13] R. E. Mulvey, D. R. Armstrong, B. Conway, E. Crosbie, A. R. Kennedy, S. D. Robertson, *Inorg. Chem.* **2011**, *50*, 12241. doi:10.1021/IC200562H
[14] E. Crosbie, A. R. Kennedy, R. E. Mulvey, S. D. Robertson, *Dalton Trans.* **2012**, *41*, 1832. doi:10.1039/C2DT11893A
[15] B. Conway, E. Crosbie, A. R. Kennedy, R. E. Mulvey, S. D. Robertson, *Chem. Commun.* **2012**, *48*, 4674. doi:10.1039/C2CC30795B
[16] M. Uchiyama, H. Naka, Y. Matsumoto, T. Ohwada, *J. Am. Chem. Soc.* **2004**, *126*, 10526. doi:10.1021/JA0473236
[17] H. Naka, M. Uchiyama, Y. Matsumoto, A. E. H. Wheatley, M. McPartlin, J. V. Morey, Y. Kondo, *J. Am. Chem. Soc.* **2007**, *129*, 1921. doi:10.1021/JA064601N
[18] H. Naka, J. V. Morey, J. Haywood, D. J. Eisler, M. McPartlin, F. García, H. Kudo, Y. Kondo, M. Uchiyama, A. E. H. Wheatley, *J. Am. Chem. Soc.* **2008**, *130*, 16193. doi:10.1021/JA804749Y
[19] H. W. Gschwend, H. R. Rodriguez, *Org. React.* **1979**, *26*, 1.
[20] V. Snieckus, *Chem. Rev.* **1990**, *90*, 879. doi:10.1021/CR00104A001
[21] M. C. Whisler, S. MacNeil, V. Snieckus, P. Beak, *Angew. Chem. Int. Ed.* **2004**, *43*, 2206. doi:10.1002/ANIE.200300590
[22] The numbering system utilised in this paper has been adopted simply to demonstrate the component parts utilised to generate the product (number = initial base, letter = Lewis donor) and does not imply that these component parts are bound to one another by a simple Lewis donor–Lewis acceptor connection.
[23] E. Crosbie, P. García-Álvarez, A. R. Kennedy, J. Klett, R. E. Mulvey, S. D. Robertson, *Angew. Chem. Int. Ed.* **2010**, *49*, 9388. doi:10.1002/ANIE.201005119
[24] R. B. Bates, L. M. Kroposki, D. E. Potter, *J. Org. Chem.* **1972**, *37*, 560. doi:10.1021/JO00969A007
[25] A. Maercker, *Angew. Chem. Int. Ed. Engl.* **1987**, *26*, 972. doi:10.1002/ANIE.198709721
[26] A. M. Corrente, T. Chivers, *Dalton Trans.* **2008**, 4840. doi:10.1039/B810319D
[27] B. Conway, J. García-Álvarez, E. Hevia, A. R. Kennedy, R. E. Mulvey, S. D. Robertson, *Organometallics* **2009**, *28*, 6462. doi:10.1021/OM900736A
[28] J. García-Álvarez, E. Hevia, A. R. Kennedy, J. Klett, R. E. Mulvey, *Chem. Commun.* **2007**, 2402. doi:10.1039/B700785J
[29] J. García-Álvarez, D. V. Graham, A. R. Kennedy, R. E. Mulvey, S. Weatherstone, *Chem. Commun.* **2006**, 3208. doi:10.1039/B606080C
[30] B. Conway, E. Hevia, J. García-Álvarez, D. V. Graham, A. R. Kennedy, R. E. Mulvey, *Chem. Commun.* **2007**, 5241. doi:10.1039/B713913F
[31] B. Conway, A. R. Kennedy, R. E. Mulvey, S. D. Robertson, J. García-Álvarez, *Angew. Chem. Int. Ed.* **2010**, *49*, 3182. doi:10.1002/ANIE.201000181
[32] H. J. Reich, W. S. Goldenberg, A. W. Sanders, *ARKIVOC* **2004**, *xiii*, 97. doi:10.3998/ARK.5550190.0005.D11
[33] G. J. P. Britovsek, J. England, A. J. P. White, *Inorg. Chem.* **2005**, *44*, 8125. doi:10.1021/IC0509229
[34] J.-C. Kizirian, N. Cabello, L. Pinchard, J.-C. Caille, A. Alexakis, *Tetrahedron* **2005**, *61*, 8939. doi:10.1016/J.TET.2005.07.008
[35] G. M. Sheldrick, *Acta Crystallogr. A* **2008**, *64*, 112. doi:10.1107/S0108767307043930
[36] P. H. Kasai, *J. Phys. Chem. A* **2002**, *106*, 83. doi:10.1021/JP013133V
[37] C. A. Bradley, L. F. Veiros, P. J. Chirik, *Organometallics* **2007**, *26*, 3191. doi:10.1021/OM0701120
[38] G. B. Deacon, P. C. Junk, G. J. Moxey, *Z. Anorg. Allg. Chem.* **2008**, *634*, 2789. doi:10.1002/ZAAC.200800238
[39] I. Korobkov, S. Gambarotta, *Inorg. Chem.* **2010**, *49*, 3409. doi:10.1021/IC902567M
[40] J. J. Fitt, H. W. Gschwend, *J. Org. Chem.* **1984**, *49*, 209. doi:10.1021/JO00175A056
[41] R. E. Mulvey, *Dalton Trans.* **2013**, *42*, 6676. doi:10.1039/C3DT00053B
[42] T. E. Barder, S. D. Walker, J. R. Martinelli, S. L. Buchwald, *J. Am. Chem. Soc.* **2005**, *127*, 4685. doi:10.1021/JA042491J